This is an unedited version of a paper accepted in **A&A**.
To be cited as: **A&A preprint doi:10.1051/0004-6361:20042247**.

Wide-band observations of the 557 GHz water line in Mars with Odin ⋆

N. Biver[1], A. Lecacheux[1], T. Encrenaz[1], E. Lellouch[1], P. Baron[1,2], J. Crovisier[1], U. Frisk[3], Å. Hjalmarson[4], M. Olberg[4], Aa. Sandqvist[5], and S. Kwok[6,7]

[1] LESIA, CNRS UMR 8109, Observatoire de Paris, 5 pl. J. Janssen, F-92190 Meudon, France
e-mail: nicolas.biver@obspm.fr
[2] Noveltis, Parc technologique du canal, 2 av. de l'Europe, 31520 Ramonville St. Agne, France
[3] Swedish Space Corporation, PO Box 4207, SE-17104 Solna, Sweden
[4] Onsala Space Observatory, SE-43992 Onsala, Sweden
[5] Stockholm Observatory, SCFAB-AlbaNova, SE-10691 Stockholm, Sweden
[6] Dept. of Physics and Astronomy, University of Calgary, Calgary, AB T2N 1N4, Canada
[7] Inst. of Astron. & Astrophys., Academia Sinica, PO Box 23-141, Taipei 106, Taiwan

Preprint online version: February 8, 2005

Abstract. The Odin satellite, thanks to the versatility of its receiver and spectrometer system, is well suited for the study of wide planetary submillimetre lines. In June and November 2003, the H_2O line at 557 GHz was observed in the Mars atmosphere over a total bandwidth of 4 GHz. The wings of the line are detected up to the nearby continuum, which provides constraints on the disc-averaged vertical thermal profile and atmospheric water mixing ratio. In parallel, a sensitive search for the O_2 line at 487 GHz was undertaken in June. This search was negative with a 3 σ upper limit of 4% on the absorption line depth, which is twice the expected signal. This observation, however, provides information on the continuum of Mars. In November the CO J(5–4) and the $H_2^{18}O$ lines were also detected in parallel and provide additional constraints on the temperature profile and mixing ratios. Surface water mixing ratios of 2–3$\times10^{-4}$ are inferred, corresponding to column densities in the range of 10–15 precipitable μm.

Key words. planets: atmospheres – planets and satellites: individual: Mars – radio lines: solar system – submillimeter

1. Introduction

Odin is an orbital submillimetre observatory (with a 1.1-m telescope) which was launched on 20 February 2001 (Nordh et al. 2003; Frisk et al. 2003). Following its in-orbit commissioning, years 2002 and 2003 were the first opportunities to make detailed studies of planetary atmospheres. Designed both for astronomy and aeronomy studies, the Odin radiometer is especially well suited for the study of planetary atmospheres.

The 2003 Mars opposition appeared as an unprecedented opportunity for Earth-based observations as Mars came at its distance closest to the Earth for centuries (0.373 AU). Earlier observations of Mars atmospheric lines around 560 GHz from space were performed in 1999 and 2001 with the Submillimeter Wave Astronomy Satellite (SWAS, Gurwell et al. 2000; Melnick et al. 2000; Gurwell et al. 2005). The 1_{10}–1_{01} transition of water at 557 GHz is very strong, which is favourable for probing the water content and its vertical distribution in the Mars atmosphere. However, the absorption line extends over more than 1 GHz. As a result, the whole profile cannot be observed with a single receiver tuning as typical bandwidths are usually 1 GHz or less. With its tunable receivers, its smaller beam and lower single sideband system temperature (T_{SYS}), Odin offers some improved capacity over SWAS for observing broad lines in planetary atmospheres.

Water vapour on Mars is known to exhibit strong seasonal and inter-annual variations, with column densities varying locally from about 1 pr-μm (precipitable micrometre) to 80 pr-μm (Jakosky and Haberle 1992; Smith 2002). H_2O was first detected long ago from the ground in the near-IR (Spinrad et al. 1963). It has been since continuously observed in the infrared

Send offprint requests to: N. Biver

⋆ Odin is a Swedish-led satellite project funded jointly by the Swedish National Space Board (SNSB), the Canadian Space Agency (CSA), the National Technology Agency of Finland (Tekes) and the Centre National d'Études Spatiales (CNES, France). The Swedish Space Corporation was the prime contractor, and is also responsible for the satellite operation.

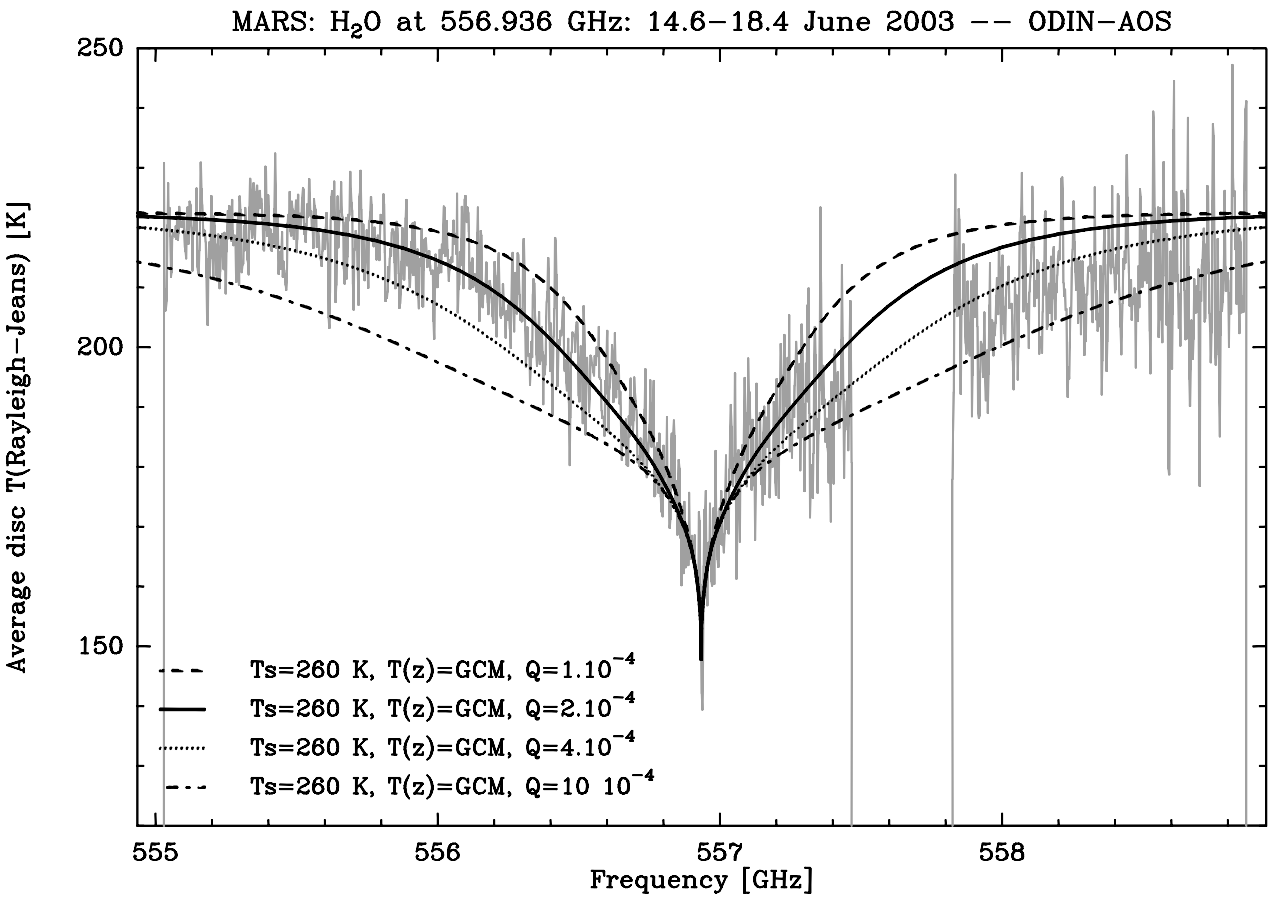

Fig. 1. The 555–559 GHz spectrum of water in Mars atmosphere in June 2003. Four 1 GHz wide AOS spectra separated by 700 MHz steps are combined. The 557.6 GHz tuning is missing due to partial failure in getting a properly tuned receiver. Corrections for beam dilution, pointing offset and beam efficiency have been applied. Average of 14–18 June observations. Four different mixing ratios (Q) with GCM temperature model (1) and T_s = 260 K surface temperature are superimposed on the spectrum. The ±1 GHz wings of the lines put significant constraints on the water mixing ratio.

range from space (Mariner 9: Conrath et al. 1973; Viking: Farmer et al. 1977; Infrared Space Observatory: Lellouch et al. 2000; Mars Global Surveyor: Smith 2002) as well as from the ground in the centimetre range (Clancy et al. 1992) and millimetre range (Encrenaz et al. 1995a, 2001). The high spectral resolution of the radio wavelength observations provides additional information through observation of pressure-broadened line profiles. Such observations can constrain the vertical distribution of water vapour and temperature. Earlier observations of water lines at 22 GHz (Clancy et al. 1992) and 183 GHz (Encrenaz et al. 1995a) from the ground have been performed, but with difficulties, due to the relative weakness of the 22 GHz line in the first case and the poor atmospheric transmission in the second case. In addition, seasonal and possibly inter-annual variations in the water mixing ratio in the Mars atmosphere are expected and justify new observations.

We report here high S/N detections with the Odin satellite of the 556.936 GHz water line in the Mars atmosphere on 14–18 June and 2–9 Nov. 2003, together with the 547.676 GHz $H_2^{18}O$ and 576.267 GHz CO lines and a sensitive search for the 487.249 GHz line of O_2. We discuss the constraints inferred on the disc-averaged water vapour content of the Mars atmosphere.

2. Observations

Mars observations were scheduled between 14 and 18 June 2003 (mean heliocentric distance: 1.419 AU) and between 2 and 9 November 2003 (mean heliocentric distance: 1.412 AU). Due to Odin elongation constraints, the planet can only be observed between elongations 60° and 120° from the Sun. Mars was closest to the Earth on 27.4 August 2003 UT, but given this constraint the best times to observe it were right before 26 June or right after 30 October 2003, when the best compromise between Mars–Earth distance and elongation restrictions was achieved. The observation log is given in Table 1 and the Mars ephemerides corresponding to the dates of observations are given in Table 2.

Figures 1 and 2 show our H_2O spectrum recorded in June, compared to different synthetic models. Figures 3 to 5 show the same line as observed in November. Figures 6 to 8 show the spectra corresponding to $H_2^{18}O$, CO and O_2 transitions, respectively.

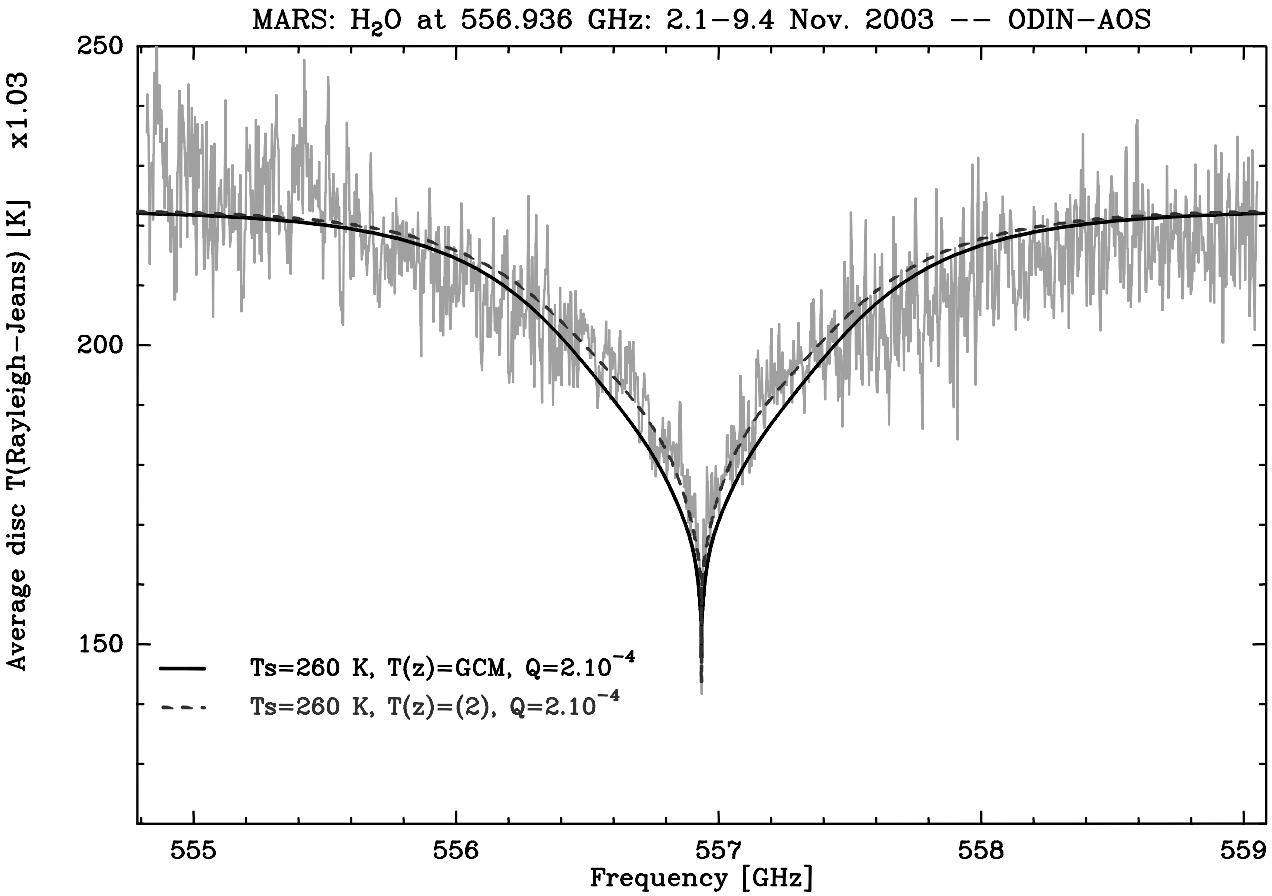

Fig. 3. The 555–559 GHz spectrum of water in the Mars atmosphere (Nov. 2003). Five 1 GHz wide AOS spectra separated by 800 MHz steps are combined. Integration time was doubled in the central part, and shortened in the 557.7 GHz tuning (Table 1). Correction for beam dilution, pointing offset and beam efficiency have been applied. Models based on temperature profiles (1, GCM) and 3, from Fig. 9, with a fixed mixing ratio (Q), are superimposed on the spectrum.

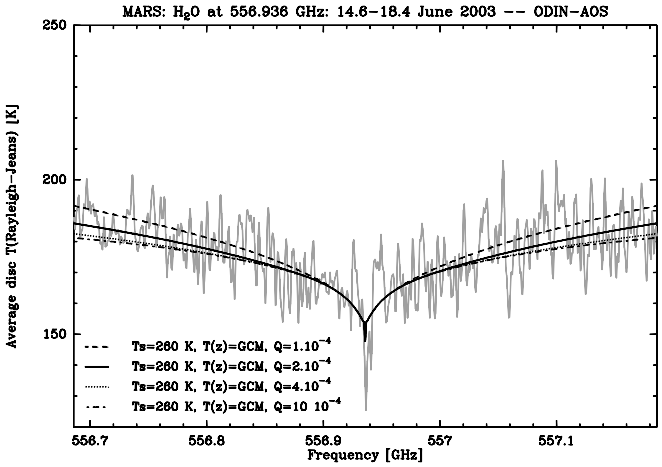

Fig. 2. The central part (700 MHz) of the spectrum of water in Mars atmosphere shown at 1.2 MHz resolution. It actually corresponds to the 14.8 June 2003 observation. Same models as for Fig. 1 are superimposed. The frequency scale has been regularly calibrated on Earth atmospheric lines and should be accurate to better than 0.1 MHz.

The basic scheme for the Mars observations was to use the Odin Dicke switching observing mode (Frisk et al. 2003), alternating between integration on the source through the main telescope beam and measuring sky noise through one of the reference sky beams, 42° away, every 3 s. In addition 2 orbits within 8 consecutive orbits were used to integrate on a reference position 15′ away from Mars in R.A.. These "OFF" position integrations were further used to properly remove instrumental effects (ripple patterns) and spillover continuum from the main beam, not subtracted in the Dicke switch process.

Due to power consumption constraints in June–July when part of the Odin orbit falls in the Earth's shadow, only 2 receivers and 2 spectrometers could be used. The "A" receiver chain was used, i.e. the 549 GHz A1 and 495 GHz A2 receivers (see characteristics in Table 3) coupled respectively with the acousto-optical spectrometer (AOS, with 1 GHz bandwidth at 1 MHz resolution and 0.6 MHz sampling) and AC1 autocorrelator set to 100 MHz bandwidth and 146 kHz effective resolution (Frisk et al. 2003).

The objectives of our observations were first to take advantage of the versatility of the system with tunable receivers to get a wide coverage in frequency of a broad planetary atmospheric (H_2O) line. In addition we attempted

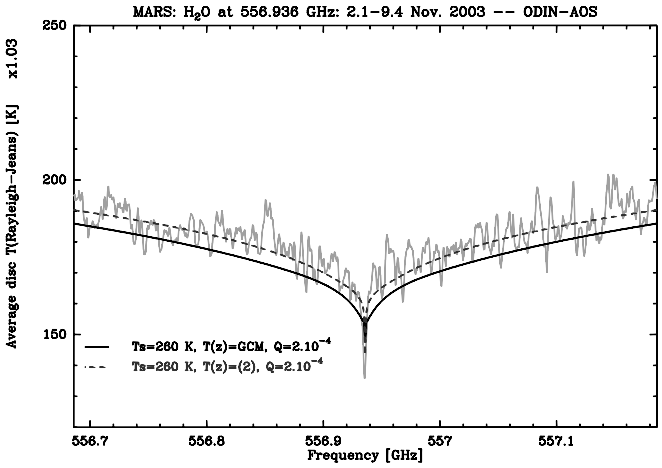

Fig. 4. Central part of the spectrum in Fig. 3, with same frequency scale as for $H_2^{18}O$ and CO lines in Figs. 6 and 7 for comparison.

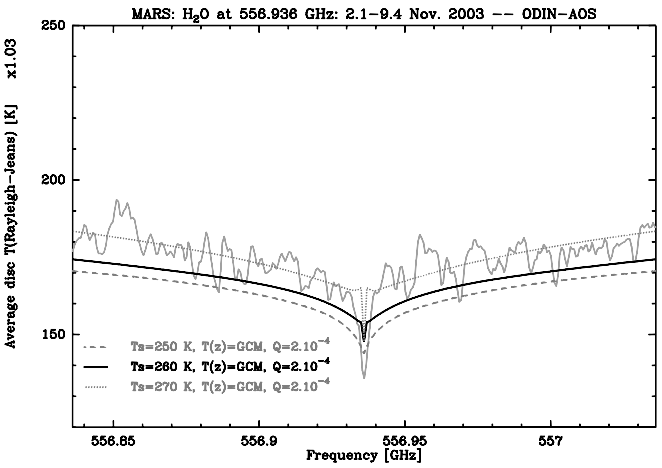

Fig. 5. Central 200 MHz of spectrum in Fig. 4. The 3 models correspond to different surface temperatures T_s=250, 260 and 270 K with same atmospheric profile and water abundance. The observed spectrum would need to be multiplied by factors 0.99, 1.03 and 1.07 respectively to fit the nearby continuum. The central peak absorption would then be slightly better modelled with the higher surface temperature, though requiring a larger correction for the continuum.

a deep integration on a molecular oxygen line, a species which has not yet been detected in any astrophysical object at radio wavelengths (i.e. with high spectral resolution). One objective of the November observations was to improve the H_2O line detection by (i) covering the missing band of June (Fig. 1), (ii) slightly improving the frequency coverage by 0.4 GHz, and (iii) using the other 555 GHz B2 receiver to avoid being on the edge of the receiver bandpass. The second objective was to use the full Odin capability to simultaneously observe the $H_2^{18}O$ line at 547.676 GHz, with the 549-A1 receiver plus AC1 autocorrelator set at 250/0.290 MHz bandwidth/resolution and the CO line at 576.267 GHz with the AC2 autocorrelator set at 500/0.580 MHz bandwidth/resolution. The $H_2^{18}O$ line provides further constraints on the water mixing ratio since it is not as optically thick as the H_2O line at 557 GHz while the CO line provides constraints on the vertical temperature profile (the mixing ratio is better known).

In order to cover the 4 GHz band spectrum of the water 556.936 GHz line displayed in Figs. 1 and 3, five different setups (5×8 orbits) with 700 MHz (800 MHz in November) steps in tuning were used. Due to the receiver 1.2 GHz instantaneous bandwidth and 1 GHz bandwidth of the AOS, a 300 MHz (200 MHz in November) overlap is obtained between each spectrum. The H_2O+700 MHz observation essentially failed in June: the receiver was not tuned for the 5 first orbits, and the reference "OFF" position ($6^{\rm th}$ orbit) was obtained before thermal equilibrium of the system was reached, especially in the case of the AOS. Mars observations obtained during this 1/3 of time are not good enough to provide constraints to the modelling, although the average continuum signal is comparable to that of H_2O-700 MHz. Besides this, a quasi perfect overlap is obtained between separately observed bands around H_2O-350 MHz and $H_2O-1050$ MHz in June and all five bands in November.

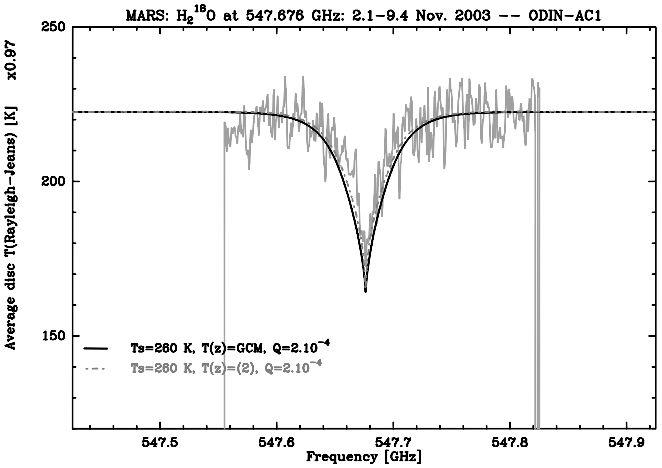

Fig. 6. Spectrum of the $H_2^{18}O$ line in Mars obtained in November. The same models as in Figs. 3 and 4 have been superimposed and provide a good fit to the observed spectra. The spectrum has been scaled up by a factor 0.97 to agree with the continuum nearby level. The AC1 autocorrelator used for this observation was the least stable spectrometer and can well explain up to 10% difference in continuum level with other spectrometers. Uncertainties in pointing and receiver beams relative offsets (on the order of 10″) and in beam efficiencies (Table 3) can also well explain differences of 5% between the continuum measured with each receiver (Figs. 3–7).

3. Data reduction

Each bin of (Signal + Reference) 2×3 s spectra has been reduced following the calibration scheme described in Olberg et al. (2003). The system temperature ($T_{\rm SYS}$) for each AOS channel has been derived from the average of all the 3×2 min per orbit calibrations, using the hot load at 283 K in the reference beam. The average $T_{\rm SYS}$ over the AOS band is given in Table 1. For the narrow

Table 1. Odin Mars observation log

Date UT yyyy/mm/dd.dd–dd.dd	orbits numbers	central [1] frequency [GHz]	Average T_{SYS} [K]	Integ. time "ON" + "OFF" [h]	Mars diameter [″]	pointing offset [″] [2]
549 A1 receiver (with AOS)						
2003/06/14.60–15.11	12560–12567	556.956 U	3080	4.8 + 1.6	14.19	4
2003/06/16.61–16.79	12590–12592	557.658 U	3200	1.6 + 0.8[3]	14.45	7
2003/06/16.81–17.19	12593–12598	558.354 U	4200	3.2 + 1.6	14.48	7
2003/06/17.21–17.32	12599–12600	558.354 U	3110	1.6 + 0	14.53	7
2003/06/17.35–17.86	12601–12608	556.254 U	3070	4.8 + 1.6	14.58	7
2003/06/17.88–18.39	12609–12616	555.558 U	3070	4.8 + 1.6	14.63	6
495 A2 receiver (with AC1)						
2003/06/14.60–15.11	12560–12567	487.254 L	2600	4.8 + 1.6	14.19	6
2003/06/16.61–18.39	12590–12616	487.254 L	2580	17.6 + 4.8	14.57	8
555 B2 receiver (with AOS)						
2003/11/02.05–02.56	14655–14663	556.936 U	3290	3.9 + 1.3	14.70	7
2003/11/02.59–03.10	14663–14671	556.140 U	3270	4.1 + 1.4	14.62	7
2003/11/03.13–03.17	14671–14672	555.335 U	3250	0.7 + 0	14.58	7
2003/11/05.61–06.05	14708–14715	555.335 U	3290	3.5 + 1.4	14.17	10
2003/11/06.08–06.32	14715–14719	557.735 U	3280	2.6 + 0.7	14.11	12
2003/11/08.29–08.30	14748–14748	557.735 U	3250	0.1 + 0	13.80	10
2003/11/08.30–08.84	14748–14756	558.540 U	3290	5.2 + 1.4	13.77	10
2003/11/08.84–09.38	14756–14765	556.940 U	3250	5.0 + 1.4	13.67	9
555 B2 receiver (with AC2)						
2003/11/08.84–09.38	14756–14765	556.936 U	3200	4.1 + 1.4	13.67	9
549 A1 receiver (with AC1)						
2003/11/02.05–02.56	14655–14663	547.676 L	3500	4.4 + 1.4	14.70	9
2003/11/05.61–06.31	14708–14719	547.676 L	3730	5.1 + 1.9	14.15	15
2003/11/08.22–09.38	14747–14765	547.676 L	3600	8.5 + 2.5	13.72	9
572 B1 receiver (with AC2)						
2003/11/02.05–03.17	14655–14672	576.268 U	3260	8.5 + 2.6	14.66	9
2003/11/05.61–06.31	14708–14719	576.268 U	3250	5.3 + 2.0	14.15	15
2003/11/08.22–08.84	14747–14756	576.268 U	3250	5.3 + 1.4	13.77	8

[1] Sky frequencies before correction for Odin velocity relative to Mars (±7 to ±33 MHz); U: upper side band, L = lower side band of the receiver.
[2] The average pointing bias provided by the attitude reconstruction versus targeted Mars position is 7″ with ≈ 5″ uncertainty in June. In addition the misalignment between the true telescope axis and the one modelled relative to the Odin platform and star-trackers is at most 15″. The 549 A1, 555 B2 and 495 A2 beams are also slightly misaligned by 7–10″ from ground measurements and ≈ 10″ in space on Jupiter maps. The difference in the continuum signal of Mars between the various frequencies can be an effect of slightly different pointing and also differences in true beam efficiencies. An additional pointing drift at the end of each orbit in June (up to 70″ for a few minutes) is not included here and apparently not well reconstructed in the attitude files.
[3] "OFF" position is at an offset of 2 to 3° instead of 15′.

band autocorrelator setup at 487 GHz, a single value over the whole 100 MHz band for T_{SYS} has been adopted (and further slope removed later, as shown in Fig. 8). This provides us with sets of ≈ 500 "ON" or "OFF" (aimed at 15′ from Mars) spectra, totaling 0.8 h integration time (Signal + Reference) per orbit.

No significant change in T_{SYS} was observed over time for any setup, except at 557 + 1.4 GHz, when a re-tuning between orbits 12598 and 12599 improved the T_{SYS} from 4200 down to 3110 K. But since the "OFF" spectra were not obtained with the same T_{SYS}, these latter data are not used in the final spectra. Using the 4200 K "OFF" reference, they do provide the same average continuum value on Mars as those obtained with T_{SYS} = 4200 K, but with a too steep slope within the band.

In each orbit, observations were actually split into 4 periods of ≈ 12 min, separated by the 2 min calibrations. Spectra for each period within an orbit are averaged after Doppler correction for the Mars velocity with respect to Odin. Then spectra from the same quarter of orbit (with similar Doppler correction) on the "OFF" position at 15′ are smoothed and subtracted from the "ON" integration. Thus all ripple patterns and the ≈ 7.8 K (13.6 K with the 555-B2 receiver) continuum from the spillover have been completely removed from Mars spectra. Results of the whole line are shown in Figs. 1 and 3.

Table 2. Mars ephemerides for the observations (from JPL Horizon server at http://ssd.jpl.nasa.gov/)

Date UT	Equatorial diameter	Geocentric distance	phase angle	Sub-Earth point long.	Sub-Earth point lat.	Sub-Solar point long.	Sub-Solar point lat.	Ls[1]
yyyy/mm/dd.dd	[″]	[AU]	[°]	[°]	[°]	[°]	[°]	[°]
2003/06/14.604	14.16	0.662	40.700	150.94	−21.15	191.61	−9.74	203.14
2003/06/15.111	14.23	0.658	40.618	328.59	−21.16	9.21	−9.87	203.45
2003/06/16.611	14.44	0.649	40.366	134.25	−21.21	174.73	−10.23	204.35
2003/06/18.396	14.70	0.637	40.047	39.71	−21.25	79.99	−10.65	205.42
2003/11/02.056	14.78	0.633	38.240	105.10	−23.70	63.26	−23.69	290.84
2003/11/03.167	14.61	0.641	38.483	134.51	−23.82	92.40	−23.57	291.51
2003/11/05.611	14.24	0.658	38.984	271.16	−24.08	228.51	−23.31	293.00
2003/11/06.313	14.14	0.663	39.120	156.96	−24.15	114.16	−23.23	293.43
2003/11/08.222	13.86	0.676	39.471	106.17	−24.35	63.00	−23.01	294.59
2003/11/09.382	13.69	0.684	39.671	152.56	−24.46	109.18	−22.88	295.29

[1] Solar longitude from the vernal point of Mars (e.g. Ls= 0° for the spring equinox of northern hemisphere and Ls= 180° for the beginning of spring in the southern hemisphere).

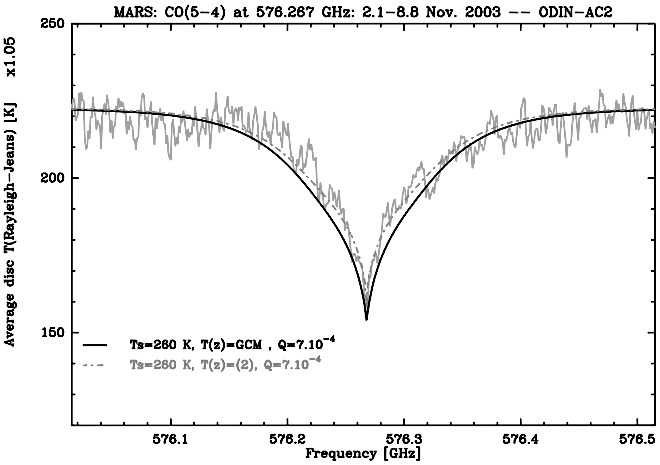

Fig. 7. Spectrum of CO line in Mars obtained in November. The same models as in Figs. 3–6 have been superimposed and provide a good fit to the observed spectrum. The spectrum has been scaled up by a factor 1.05 (See Fig. 6 for explanations). The width of the spectrum is 500 MHz as in Figs. 4 and 6, for comparison.

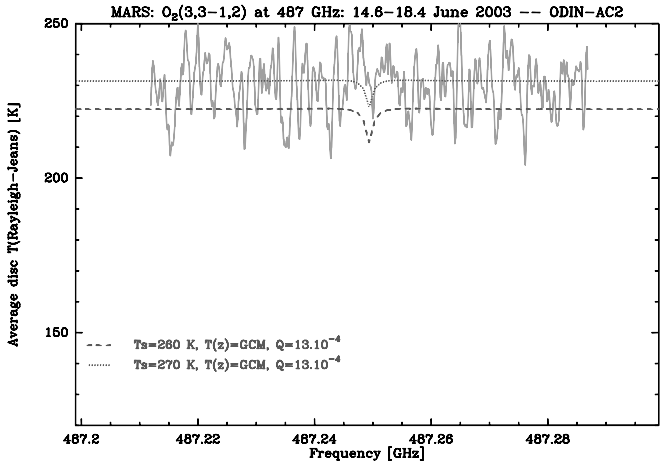

Fig. 8. The 487.2 GHz integration spectrum in Mars centred on the O_2 line. All the observations have been used with an average pointing offset estimated to 15″. Pointing, beam dilution and efficiency corrections have been applied to retrieve the disc-averaged Rayleigh-Jeans temperature $T_{\rm RJ}$ and a curvature in the continuum coming from non-uniform $T_{\rm SYS}$ across the band has been removed. Models with the expected line and continuum intensity ($T_{\rm s}$ = 260 K and 270 K, see text) have been superimposed.

Larger pointing offsets occurred during the last quarter of all June orbits (yielding a continuum level about 25% lower or 12% lower at 487 GHz). Such a problem is often due to the use of only one of the two star trackers. For this reason only the 3 first quarters of the orbits have been used to make the Figs. 1–5 spectra. Spectra were then converted from the antenna temperature scale into disc average Rayleigh-Jeans temperature. This is done in three steps: (i) correcting for the main beam efficiency of Odin with values from Table 3 which have been measured independently on Jupiter at several opportunities (Frisk et al. 2003); (ii) correcting for the small losses due to pointing offsets from Table 1; (iii) and then dividing by the beam dilution factor computed from Odin beam size and Mars apparent diameter at the time of each observation given in Tables 1 and 3. Up to now the image band gain (G_i) has been considered as negligible (below 1%) but it was estimated to be higher (6–8%) from contemporaneous Earth atmospheric lines observation. This is actually more the case for the off-line setup (frequencies offset from the 556.9 GHz central frequency of the water line) for which the image band rejection filter was less optimized. The impact on the spectra is negligible, especially for continuum measurements: to take this into account, the spectra should first be multiplied by a factor $1+G_i$ (due to underestimation of the $T_{\rm SYS}$) and then the fraction (signal×gain) of the continuum signal coming from the image sideband has to be subtracted. This would not change the continuum level and would increase the contrast of the lines by a factor $1+G_i$. In the worst case the depth of the water line is underestimated by 4

Table 3. Telescope and receiver tuning characteristics

Receiver	Frequency [GHz]	θ_B [1] ["]	η_{mB} [2]	G_i [3]
495 A2	487.3	146	0.92 ± 0.02	≈ 0.03
549 A1	557	127	0.84 ± 0.03	0.04
	555–556	128	0.84 ± 0.03	0.06
	558.3	127	0.83 ± 0.03[4]	0.06
	547.7	130	0.85 ± 0.03	< 0.03
555 B2	557	127	0.87 ± 0.03	< 0.02
	555–556	128	0.87 ± 0.03	0.08
	558–559	127	0.87 ± 0.03	0.06
572 B1	576.2	124	0.85	< 0.06

[1] Main beam FWHM.
[2] Main beam efficiency value estimated from previous Jupiter maps.
[3] Image band gain estimated from telluric lines observed in image bands during Earth limb crossing/calibration.
[4] The 558 GHz tuning (554 GHz LO frequency) is at the edge of the total bandwidth (17 GHz centred at 549 GHz) of the receiver and its performance is slightly degraded.

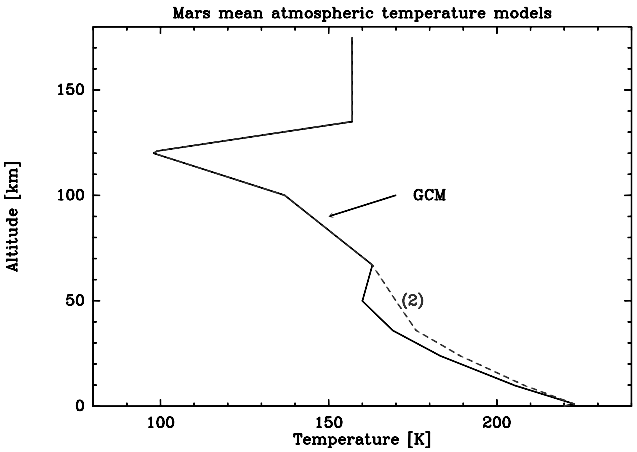

Fig. 9. Different thermal vertical profiles of the Mars atmosphere used in Figs. 1 to 7: Temperature profile (1) is the GCM with a temperature inversion around 60 km. Profile (2) is the GCM with higher temperature at lower altitude, used in Figs. 3 to 7.

K. These spectra can then be directly compared to the model of the Rayleigh-Jeans temperature ($T_{\rm RJ}$) averaged over the whole disc of Mars that fitted well within the beam (Section 4). Note that at 560 GHz $T_{\rm RJ}$ is about 13 K lower than the brightness Planck temperature.

4. Modelling of Martian atmospheric lines and results

4.1. Surface temperature and atmospheric models

Synthetic spectra corresponding to the observing conditions and averaged over the whole disc of Mars have been calculated and superimposed in Figs 1–8. They are computed from a mean atmospheric vertical temperature profile and a surface temperature averaged over the whole disc. According to the Mars Global Climate Model (GCM; Forget et al. 1999) for Ls= 204.6°, the mean surface pressure is 5.18 mbar and the mean surface temperature is $T_{\rm s}$ = 245.6 K (with strong local variations, ranging from 147 to 299 K). For November, conditions were very similar: $T_{\rm s}$ local variations were between 150 and 300 K, the mean surface pressure was 5.19 mbar and GCM thermal profile was also very similar. Thus we adopted the same modeling for both periods – the differences being not noticeable with these observations. Values actually measured for the atmospheric temperature by the TES experiment on Mars Global Surveyor completely agree with the GCM model used here.

Beam efficiency and pointing uncertainties (Sect. 3, and Frisk et al. 2003) can give up to 7% uncertainty in the continuum level – justifying the multiplying factors of up to 1.07 in Figs 3–7. The observing scheme and AOS absolute calibration should be reliable while autocorrelators can be less accurate for determining continuum values. Taking into account the 487 GHz measurement (Fig. 8, Table 1) which is less sensitive to pointing offsets and far from broad lines, we get an average Rayleigh-Jeans temperature of 230 ± 4 K, requiring a surface temperature $T_{\rm s} = 268 \pm 5$ K. The continuum measured on the wings of the other lines is $T_{\rm RJ} = 221 - 212$ K from H_2O in June, $T_{\rm RJ} = 217 \pm 4$ K, 228 K and 210 K respectively for November H_2O, $H_2^{18}O$ and CO data. The average is close to 221 K which converts into a surface temperature of 260 K (assuming 0.9 emissivity and taking into account the Rayleigh-Jeans to Planck temperature correction). The small multiplying factors used in Figs 3–7 bring the continuum of these spectra to 221 K. Recent in-orbit measurements by the Mars Global Surveyor also point towards such a relatively high temperature and we adopted a surface temperature of 260 K for the models.

In Fig. 5 we plotted the result of a 10 K variation of $T_{\rm s}$ (models 6 and 7 from Table 4): if one makes a corresponding correction to the spectra, a slightly higher $T_{\rm s}$ can also provide a good fit, without much changing the results in term of water abundance. Several small variations from the GCM in the vertical atmospheric temperature profiles have been tested and one is given in Fig. 9. Table 4 summarizes the various models used to fit the observed lines and that are superimposed on the spectra.

4.2. H_2O line

The observing scheme we used removed most of the ripple pattern, and provided a smooth baseline and a wide frequency coverage (3.9 and 4.2 GHz versus 0.6 GHz in the case of SWAS). This enables us to see the whole line up to the nearby continuum and provides better constraints on the global vertical temperature profile and water content of the Mars atmosphere at the time of the observations (southern hemisphere spring in June 2003 and southern hemisphere summer in November 2003; Table 2).

The Mars absorption line was modeled using the code described by Encrenaz et al. (1995a). Our synthetic mod-

Table 4. Temperature and atmospheric models

Model			Water vapour		Figs.
	T_s [K]	$T(z)$[1]	mixing ratio		
1	260	GCM	1×10^{-4}	(5.9 pr-μm)[2]	1,2
2	260	GCM	2×10^{-4}	(11.5 pr-μm)	1–8
3	260	GCM	4×10^{-4}	(22.2 pr-μm)	1,2
4	260	GCM	10×10^{-4}	(51.2 pr-μm)	1,2
5	260	(2)	2×10^{-4}	(11.5 pr-μm)	3,4, 6,7
6	250	GCM	2×10^{-4}	(11.5 pr-μm)	5
7	270	GCM	2×10^{-4}	(11.5 pr-μm)	5,8

[1] Atmospheric vertical temperature profile from Fig. 9.
[2] micrometres of precipitable water.

els are listed in Table 4. We first assumed the GCM thermal profile with a mean surface temperature of 260 K and investigated different values of the surface mixing ratio (models 1–4). As shown in Fig. 1, values of 2–3 $\times 10^{-4}$ (model 2) are required to fit the far wings, but the synthetic spectrum is still above the observed one in the core of the line (Fig. 2). Varying mixing ratios were also investigated for November data, and $Q = 2 \times 10^{-4}$ was found to be a good compromise. Models 2 and 5 for November were calculated using $T_s = 260$ K and the GCM temperature profile (1) or with a warmer lower atmosphere (model 5 with temperature profile (2) from Fig. 9) which further improve the quality of the fit to the line wings (Fig. 3). Using the wings (Figs 1 and 3) and the central part (Figs 2 and 4) of the line, we infer a H_2O surface mixing ratio of 2–3 $\times 10^{-4}$, which corresponds to H_2O column densities ranging from 10 to 15 pr-μm.

4.3. $H_2^{18}O$ line at 547.676 GHz

This line corresponds to the same fundamental rotational ortho transition ($1_{10} - 1_{01}$) as the water line at 557 GHz. It was previously detected in 2001 in Mars with SWAS (Gurwell et al. 2005). The good S/N detection of this $H_2^{18}O$ line in the atmosphere of Mars provides further constraints on its water content. But given the high $H_2^{16}O/H_2^{18}O$ ratio close to 500 (roughly terrestrial) – suggested by independent observations of Mars (as reviewed by Owen (1992)) – only the central part of the line is seen, corresponding to the saturated case for $H_2^{16}O$ (Figs 4 and 6 plotted with the same frequency and temperature scale). The absorption line is clearly detected in November and the synthetic spectra from models 2 and 5 (Table 4) provide a good fit (Fig. 6) to the observation. The line strength is actually nearly proportional to the water abundance and provides a better constraint than the saturated H_2O line. We can see from Fig. 6 that a 20% increase or decrease in the line strength would provide a significantly poorer fit. When minimizing the difference between the observation and the model the residuals stay within the noise for a H_2O surface mixing ratio of $1.8 \pm 0.3 \times 10^{-4}$ (9–12 pr-μm), probably slightly lower than in June. Increasing T_s to 270 K would slightly improve the fit, yielding a similar H_2O mixing ratio (about 1.7×10^{-4}).

4.4. CO line at 576.267 GHz

CO millimetre to sub-millimetre lines have been regularly observed in Mars from the ground. Here, the $J = 5 - 4$ line at 576.267 GHz could be observed with Odin in parallel to the water lines. It provides measurement of the continuum at another frequency, although it is more sensitive to pointing errors and the autocorrelator data, especially for the AC1 used for $H_2^{18}O$, are more prone to continuum level uncertainty due to platforming problems. Changing the surface temperature to 250 K or 270 K will not significantly change the line shape and contrast. The CO line profile provides a determination of the temperature profile at the same time as the water observations. Given the chemical stability of CO and its long lifetime, the CO column density is expected to be constant with time. Thus the CO mixing ratio is expected to show moderate (30%) variations anticorrelated with the pressure cycle. We adopted here a standard 7×10^{-4} (Lellouch et al. 2000) CO mixing ratio. The impact of the precise CO mixing ratio on the temperature retrieval is small given that the strongly saturated CO J(5–4) line is much more sensitive to the temperature than to the CO mixing ratio. In addition, as discussed in Sect.4.1, the temperature profile appears to be very consistent, to within a few degrees, with mean temperatures retrieved concomitantly with MGS-TES. From Fig. 7, we can see a good agreement with temperature profile (1) and (2) from Fig. 9, the latter one providing a slightly better fit.

4.5. O_2 at 487.249 GHz

The $N_J = 3_3 - 1_2$ line of O_2 at 487.249 GHz was not detected (Fig. 8). The 3 sigma contrast limit is 4.2% relative to the Mars continuum for a 4 MHz width (rms = 6.3 K at 1 MHz resolution). Oxygen in the Mars atmosphere was observed by visible spectroscopy and *in situ* mass spectrometry giving a mixing ratio of 0.0013. Modelling by Encrenaz et al. (1995b) predicted a line in absorption somewhat weaker (2%–2.5% for a 4 MHz resolution), which is compatible with our observations. Our observations would have been sensitive to a O_2 abundance 2–3 times higher. Future heterodyne detection of Martian O_2 will await the availability of Herschel/HIFI which could search for the more favourable $N_J = 7_6 - 5_6$ line at 1121 GHz (Encrenaz et al. 2004).

5. Discussion and conclusions

Our observations have allowed the first complete spectrally resolved measurement of a strong water vapour transition in the Martian atmosphere. They provide new constraints on the H_2O mean abundance and vertical distribution. However, both the thermal profile

and the water vapour vertical distribution are known to exhibit strong variations over the Martian disc (Jakosky and Haberle 1992; Smith 2002), and the disc-averaged information retrieved from our data must be taken carefully. In particular, the fact that we infer (both from our calibration and from modelling) a mean surface temperature higher than expected from the GCM might be due to the very large variations of this parameter over the Martian disc.

We find that a H_2O surface mixing ratio of the order of $2–3 \times 10^{-4}$ in June and 1.8×10^{-4} in November gives the best fits to our data, corresponding to water vapour column densities of about 13±3 and 10±2 pr-μm respectively. These values are consistent with the estimate (about 10–15 and ≈ 5 pr-μm, respectively) inferred from the Viking observations for the southern hemisphere spring and summer in the range of 0–40° southern latitudes (Jakosky and Haberle 1992). More recent TES data from the Mars Global Surveyor (Smith 2002) are also in agreement with ours, this time from the higher side (15–20 and ≈15 pr-μm for $Ls = 205°$ and 293°). We note that our determination of the water vapour content is comparable to the measurements based on SWAS observations of the same H_2O transition. In 1999 (Gurwell et al. 2000) the SWAS observations took place at $Ls = 130°$, corresponding to mid-northern summer. The SWAS determination, (8 $+12/-3$ pr-μm), is lower than the expected Viking value for this season (about 20 pr-μm between 0 and 40° northern latitudes (Jakosky and Haberle 1992). This was explained by a saturation effect at about 10 km, the temperature profile being colder than expected from the GCM. The 2001 value obtained by SWAS (12 ± 6 pr-μm, for $Ls = 166 - 233°$) is very similar to our June 2003 determination. In our calculations, the saturation effect is less sensitive, as, in the case of our best-fit model ($Q = 2–3 \times 10^{-4}$ with the GCM thermal profile), saturation takes place at an altitude of 22 km. The simultaneous observation of the 557 GHz H_2O and 548 GHz $H_2^{18}O$ lines and the CO $J(5–4)$ transition with Odin in November provides further validation of the model used, constraining simultaneously the thermal profile and the water vapour vertical distribution.

Acknowledgements. Generous financial support from the Research Councils and Space Agencies of Canada, Finland, France and Sweden is gratefully acknowledged. We thank the referee Mark Gurwell for his fruitful remarks to improve the paper and for his providing of the latest SWAS Mars results ahead of final publication. We also thank Mike Smith for providing us with detailed information on MGS-TES measurements at the time of Odin observations.

References

Conrath, B., Curran, R., Hanel, R. et al., 1973, J. Geophys. Res., 78, 4267
Clancy, R.T., Grossman, A.W., and Muhleman D.O., 1992, Icarus, 100, 48
Encrenaz, T., Lellouch, E., Cernicharo, J. et al. 1995a, Icarus, 113, 110
Encrenaz, T., Bézard, B., Crovisier, J. et al. 1995b, Planet. Space Sci., 43, 1485
Encrenaz, T., Lellouch, E., Paubert, G. and Gulkis, S., 2001, Planet. Space Sci., 49, 731
Encrenaz, T., Lellouch, E., Atreya, S.K. and Wong, A.S., 2004, Planet. Space Sci., 52, 1023
Farmer, C.B., Davies, D.W., Holland, A.L., Laporte, D.D. and Doms P.E. 1977, J. Geophys. Res., 82, 4225
Forget, F., Hourdin, F., Fournier, R. et al. 1999, J. Geophys. Res., 104-E10, 24155
Frisk, U., Hagström, M., Ala-Laurinaho, J. et al. 2003, A&A, 402, L27
Gurwell, M.A., Bergin, E.A., Melnick, G.J. et al. 2000, ApJ, 539, L143
Gurwell, M.A., Bergin, E.A., Melnick, G.J. and Tolls, V., 2005, Icarus, *in press*
Jakosky, B.M. and Haberle, R.M., 1992, In: Mars, H.H. Kieffer et al. edts, University of Arizona Press, 969
Lellouch, E., Encrenaz, T., de Graauw, T. et al. 2000, Planet. Space Sci., 48, 1393
Melnick, G.J., Stauffer, J.R., Ashby, M.L.N. et al. 2000, ApJ, 539, L77
Nordh, H.L., von Schéele, F., Frisk, U. et al. 2003, A&A, 402, L21
Olberg, M., Frisk, U., Lecacheux, A. et al. 2003, A&A, 402, L35
Owen, T., 1992, In: Mars, H.H. Kieffer et al. edts, University of Arizona Press, 818
Smith, M.D., 2002, J. Geophys. Res., 107-E11, 25
Spinrad, H.G., Munch. G. and Kaplan, L.D. 1963, ApJ, 137, 1319